Réf II.5

C. R. Acad. Sci. Paris, t. 316, Série II, p. 1695-1702, 1993

Acoustique/*Acoustics*

Arrival-time variance for acoustic propagation in 3-D random media: the effect of lateral scales

Michael J. KARWEIT and Philippe BLANC-BENON

Abstract – In a series of numerical simulations following acoustic rays propagating through ensembles of 3-D, random, isotropic, inhomogeneous fields, we demonstrate that the travel-time variance for rays travelling a fixed distance is systematically different depending on whether the rays are travelling through velocity or temperature fields.

Conjecturing that these differences are related to the differences in lateral scales of the derived perturbation fields we try to match the perturbation fields by constructing axisymmetric, "vector-equivalent" scalar (temperature) fields which match the lateral Taylor microscales λ_2 and longitudinal integral scales L_f of comparable isotropic velocity fields. Travel-time variance through these axisymmetric scalar fields is found to approach that of the vector fields, suggesting that lateral scales do play an important role; but that λ_2 may not be the best lateral measure.

Influence des échelles latérales sur la variance du temps de parcours des ondes acoustiques dans un milieu aléatoire tridimensionnel

Résumé – *Dans cette analyse nous présentons une série de simulations numériques de la propagation d'une onde acoustique à travers une turbulence tridimensionnelle cinématique ou thermique. Nous démontrons que la variance des fluctuations de temps de parcours le long des rayons pour une distance source récepteur fixe est très fortement dépendante du caractère scalaire ou vectoriel des fluctuations aléatoires du milieu. Nous illustrons également l'importance d'une prise en compte des échelles latérales du champ turbulent dans une description théorique.*

Version française abrégée – Les ondes acoustiques qui se propagent dans un milieu turbulent subissent d'importantes perturbations dues aux fluctuations aléatoires du milieu. Pour une source et un récepteur séparés d'une distande d, les modifications des propriétés spatio-temporelles du champ acoustique propagé se traduisent notamment par une fluctuation du temps de parcours. Dans le cadre de la théorie des rayons, la relation (1) proposée par Chernov (1960) permet de calculer la variance du temps de parcours $\langle t'^2 \rangle$ à partir de la variance des fluctuations d'indice du milieu $\langle \mu^2 \rangle$ et d'une échelle longitudinale de turbulence L_f. Dans le cas d'un champ de fluctuations thermiques $T'(x)$ nous avons $\mu(x) \approx -.5\,T'(x)/T_0$, où T_0 est une température de référence. Pour une turbulence cinématique $\mathbf{u}(x)$, si x_1 est la direction de l'onde incidente, on montre que $\mu(x) \approx -u_1(x)/c_0$, où c_0 est la célérité du son en l'absence de fluctuation du milieu (Candel, 1979).

Karweit *et al.* (1991) ont introduit une approche nouvelle du problème à partir d'une simulation numérique scindée en deux étapes successives : d'abord la génération d'un champ aléatoire (scalaire ou vectoriel) homogène et isotrope par superposition d'un ensemble fini de modes de Fourier aléatoires de caractéristiques spectrales connues, et ensuite la résolution des équations de propagation des rayons déduites de l'acoustique géométrique. Le temps de traversée de la turbulence par l'onde acoustique est nettement inférieur au temps d'évolution des champs turbulents, ce qui permet de faire une hypothèse de turbulence gelée. Les équations de propagation des rayons acoustiques pour un milieu inhomogène en mouvement et indépendant du temps sont alors données par les relations (2) et (3). Le milieu aléatoire de propagation est simulé avec 60 modes de Fourier équirépartis entre $k_{min} = 1\ m^{-1}$ et $k_{max} = 60\ m^{-1}$, de directions angulaires aléatoires dans l'espace spectral. L'amplitude de chaque mode de Fourier [$E(k)^{1/2}$ pour un champ vectoriel et $G(k)^{1/2}$ pour un champ scalaire]

Note présentée par Geneviève COMTE-BELLOT.

0764-4450/93/03161695 $ 2.00

est fixée à partir d'une répartition spectrale de l'énergie turbulente. Pour chaque réalisation le système d'équations différentielles est intégré numériquement en utilisant une méthode de Runge-Kutta d'ordre 4 (Karweit, 1991). Le champ acoustique transmis est ensuite caractérisé par des moyennes statistiques sur un ensemble de réalisations.

Les résultats obtenus concernent des champs aléatoires homogènes et isotropes pour lesquels les amplitudes $E(k)^{1/2}$ et $G(k)^{1/2}$ sont données par les relations (5) et (6), et correspondent à une fonction de corrélation spatiale des fluctuations de vitesse ou de température gaussienne $\rho(r)=e^{-r^2/l^2}$. Pour chacune des simulations la distance maximale de propagation dans la turbulence est égale à 40 fois l'échelle intégrale L_f avec $L_f=\int_0^\infty \rho(r)\,dr=1\sqrt{\pi}/2$. Nous utilisons une échelle de longueur l de 0,1 m et trois taux de fluctuations d'indice différents $\langle \mu^2 \rangle^{1/2}=\mu_0$, $2\mu_0$, et $4\mu_0$, avec $\mu_0=2/340$. Les moyennes sont calculées avec 1 000 réalisations.

Sur la figure 1, nous avons tracé la variance des fluctuations de temps de parcours $\langle t'^2 \rangle$ en fonction de la distance source-récepteur d normalisée par l'échelle intégrale L_f. Pour chaque courbe nous avons également normalisé la variance $\langle t^2 \rangle$ par la valeur théorique fournie par la relation de Chernov à $d=40\,L_f$. Nous remarquons que l'écart avec la solution de Chernov est très important dès que $d/L_f \geqq 10$. Cet écart augmente avec la distance de propagation et le niveau des fluctuations d'indice. On observe aussi que les champs aléatoires de vitesse et de température ne fournissent pas quantitativement les mêmes variances de temps de parcours pour la même fonction de corrélation spatiale des fluctuations d'indice. Cette différence peut sans doute s'expliquer par le fait que les échelles de longueur associées aux gradients transversaux responsables de la courbure des rayons acoustiques dépendent du caractère scalaire ou vectoriel du champ turbulent simulé. En effet si l'échelle intégrale longitudinale L_f est la même pour les deux champs, les échelles latérales diffèrent, et notamment les échelles de Taylor λ_i définies par la relation (7). Pour un champ scalaire nous avons $\lambda_2=\lambda_3=\lambda_1$ tandis que pour un champ vectoriel cette relation devient $\lambda_2=\lambda_3=\lambda_1/\sqrt{2}$.

Pour mettre en évidence les effets des échelles de Taylor transversales par rapport à la direction de propagation de l'onde acoustique, nous avons simulé un champ scalaire anisotrope (axisymétrique) pour lequel les échelles L_f et λ_i sont identiques à celles d'un champ de vitesse isotrope. Pour cela nous utilisons la théorie linéaire de la distortion rapide [Batchelor (1953)] en soumettant le champ de température initialement isotrope à une contraction de rapport C, ce qui modifie les échelles de turbulence dans les rapports donnés par les relations (9) et (10). Sur la figure 2 on observe une évolution similaire de la variance $\langle t'^2 \rangle$ avec la distance d pour les deux types de champs turbulents, mais avec un écart d'autant plus réduit que le niveau des fluctuations d'indice μ_0 est élevé. A titre d'exemple nous avons indiqué par une barre verticale, sur chacune des figures, l'écart entre les simulations obtenues pour $2\mu_0$ à la distance $d=20\,L_f$. Il convient de noter également que la solution classique de Chernov, qui ne prend pas en compte les effets des échelles latérales des fluctuations d'indice, est totalement mise en défaut pour les distances de propagation importantes ($d/L_f \geqq 10$). A partir des travaux de Blanc-Benon (1991) sur la focalisation en milieu aléatoire, une analyse plus fine des effets dus aux échelles transversales des fluctuations de vitesse et de température est actuellement en cours.

INTRODUCTION. – One of the characteristics of an acoustic wave propagating through an inhomogeneous medium is loss of phase coherence. That is, the time it takes for

points of constant phase along an acoustic wavefront to travel a fixed distance d is not constant. Chernov (1960) considered this problem for acoustic propagation through a weakly inhomogeneous velocity field in the case where the ray model was valid. He assumed that in such a field, an acoustic ray would closely follow its initial direction of propagation, and hence would depend on the field only along that line. This assumption permitted him to characterize an average influence of a field in terms of its integral length scale L_f. Chernov thus deduced the average travel-time variation to be:

$$\langle t'^2 \rangle = 2 L_f \langle \mu^2 \rangle d/c_0^2, \tag{1}$$

where $\langle \mu^2 \rangle$ is the mean-square value of the perturbation field $\mu(\mathbf{x})$, d is the distance of propagation, and c_0 is the average sound speed of the medium. For a ray travelling primarily in the x_1 direction in an inhomogeneous velocity field $\mathbf{u}(\mathbf{x})$, $\mu(\mathbf{x}) \approx -u_1(\mathbf{x})/c_0$ (Candel, 1979). In a temperature field, $\mu(\mathbf{x}) \approx -.5\, T'(\mathbf{x})/T_0$, where T_0 is some reference temperature.

Karweit *et al.* (1991) carried out a series of numerical simulations of rays propagating through Fourier-synthesized velocity fields and verified the Chernov result, but only when rays were not permitted to deviate from their initial direction of propagation. Using the full ray-trace equations expressed by Candel (1977) or by Pierce (1981), and not restricting the direction of the trajectories, they found that the phase variance exceeded the Chernov prediction.

The present paper extends the work of Karweit (1991) and reports on significant differences between acoustic propagation in vector (velocity) fields and in scalar (temperature) fields with the same values of the mean-square perturbation field $\langle \mu^2 \rangle$ and integral length scale L_f. We demonstrate that not only these differences, but also the deviations from the Chernov prediction, are largely attributable to the influence of the lateral scales of inhomogeneity of the medium.

SIMULATING THE TRAJECTORY OF AN ACOUSTIC RAY THROUGH AN INHOMOGENEOUS FIELD. — Like Karweit (1991), here we follow the trajectory of a phase point on an acoustic wave through an inhomogeneous field with soundspeed $c(\mathbf{x})$ and velocity fluctuation $\mathbf{u}(\mathbf{x})$ by numerically integrating the ray-trace equations. These equations, taken from Pierce (1981), incorporate an auxiliary "slowness" vector $\mathbf{s}$, so that all terms of the equations can be expressed entirely as a function of the field and its gradients:

$$\frac{dx_i}{dt} = \frac{c^2 s_i}{\Omega} + u_i \tag{2}$$

$$\frac{ds_i}{dt} = -\frac{\Omega}{c}\frac{\partial c}{\partial x_i} - \sum_{j=1}^{3} s_j \frac{\partial u_j}{\partial x_i} \tag{3}$$

where $\Omega = 1 - \mathbf{u}.\mathbf{s}$; x_i is the ith coordinate of a phase point; and s_i is the ith component of the associated slowness vector.

The inhomogeneous velocity and/or temperature field is prescribed as a superposition of randomly-oriented Fourier modes so the spatial derivatives of the field can be deduced analytically. Thus no numerical approximations are required for expressing the right-hand-sides of the equations. At time $t=0$, a phase point on a wavefront is assumed to start at $\mathbf{x}=0$ propagating away from the origin, initially in the x_1 direction. Its trajectory is deduced by integrating the ray-trace equations forward in time using a 4th-order Runge-Kutta time-step scheme. At a prescribed radial distance d from the origin, the phase point's travel time is recorded. Computations are carried out in double precision

with an integration time step of $\Delta t = 1./(c_0 k_{max})$ the longest step for which results duplicate those obtained from integrations of half that step size. This is the same criterion for stepsize that was used in Karweit (1991) and Blanc-Benon (1990). Here, k_{max} is the upper limit of the wavenumber in the discretization of the turbulent spectrum.

This procedure is then repeated over an ensemble of statistically similar fields to provide data for estimating travel time variance. During the integration of a trajectory, the travel time is so short compared to any dynamic time scale of a physical field, that we make the assumption that the field is "frozen". Further, since the Fourier wavevectors comprising the fields are non-integrally related, the fields are non-periodic and of infinite extent.

In the present study, each realization of a random field is based on 60 Fourier wavevectors whose magnitudes are equally spaced between wavenumber $k_{min} = 1\ m^{-1}$ and $k_{max} = 60\ m^{-1}$ and whose directions are randomly distributed in 3-space. The contribution of each Fourier mode, $E(k)^{1/2}$ for vector fields and $G(k)^{1/2}$ for scalar fields, is related deterministically to a prescribed wavenumber spectrum yielding both the spatial scales and perturbation indices of the fields.

For all experiments, we prescribe fields having an average velocity of zero and/or an average temperature of T_0. Inhomogeneities are statistically described in terms of an isotropic spatial correlation function $\rho(r) = \langle T'(\mathbf{x}+\mathbf{r}) T'(\mathbf{x}) \rangle / \langle T'^2(\mathbf{x}) \rangle$, where $T'(\mathbf{x}) = T(\mathbf{x}) - T_0$. For velocity fields $\rho(r) = \langle u_i(\mathbf{x}+r_i) u_i(\mathbf{x}) \rangle / \langle u_i^2(\mathbf{x}) \rangle$ is the correlation of the velocity components in the direction of the separation r, and is referred to in the turbulence literature as $f(r)$. For isotropy, $\langle u_i^2(\mathbf{x}) \rangle = \text{Const.}$ for any i. We choose $\rho(r)$ to be Gaussian and to depend on the single length scale l:

$$\rho(r) = e^{-r^2/l^2}. \tag{4}$$

This correlation function transforms into three-dimensional energy spectra as:

$$E(k) = \frac{1/3 \langle u^2 \rangle k^4 l^5}{8\sqrt{\pi}} e^{-k^2 l^2/4} \tag{5}$$

$$G(k) = \frac{\langle T'^2 \rangle k^2 l^3}{2\sqrt{\pi}} e^{-k^2 l^2/4} \tag{6}$$

for velocity and temperature fields, respectively (Hinze, 1975). k is the wavenumber, and $\langle T'^2 \rangle$ and $\langle u^2 \rangle = \langle u_1^2 + u_2^2 + u_3^2 \rangle$ are the mean square temperature and velocity inhomogeneities averaged over the fields. The integral length scale is computed as

$$L_f = \int_0^\infty \rho(r)\, dr = l\sqrt{\pi}/2,$$

and the mean square perturbation index becomes $\langle \mu^2 \rangle = \langle T'(\mathbf{x})^2 \rangle / (2T_0)^2$ for temperature fields, and $\langle \mu^2 \rangle = \langle u_1(\mathbf{x})^2 \rangle / c_0^2$ for velocity fields (where acoustic propagation is primarily in the x_1 direction). c_0 and T_0 are reference sound speed and temperature, and are taken as $c_0 = 340$ m/s and $T_0 = 300$ K.

Our numerical experiments consisted of following the trajectories of phase points propagating through each of an ensemble of 1,000 independent, statistically-similar, random inhomogeneous fields, and then recording travel-time as a function of radial distance travelled. This provided the data to compute travel-time variance.

NUMERICAL EXPERIMENTS ON SCALAR AND VECTOR FIELDS. – Six experiments were performed initially – three with temperature fields, three with velocity fields – all having the

same length parameter $l=0.1$ m (*i.e.* $L_f=0.1\sqrt{\pi}/2$), but having several different perturbation indices: $\langle \mu^2 \rangle^{1/2}=\mu_0$, $2\mu_0$, and $4\mu_0$, with $\mu_0=2/340$.

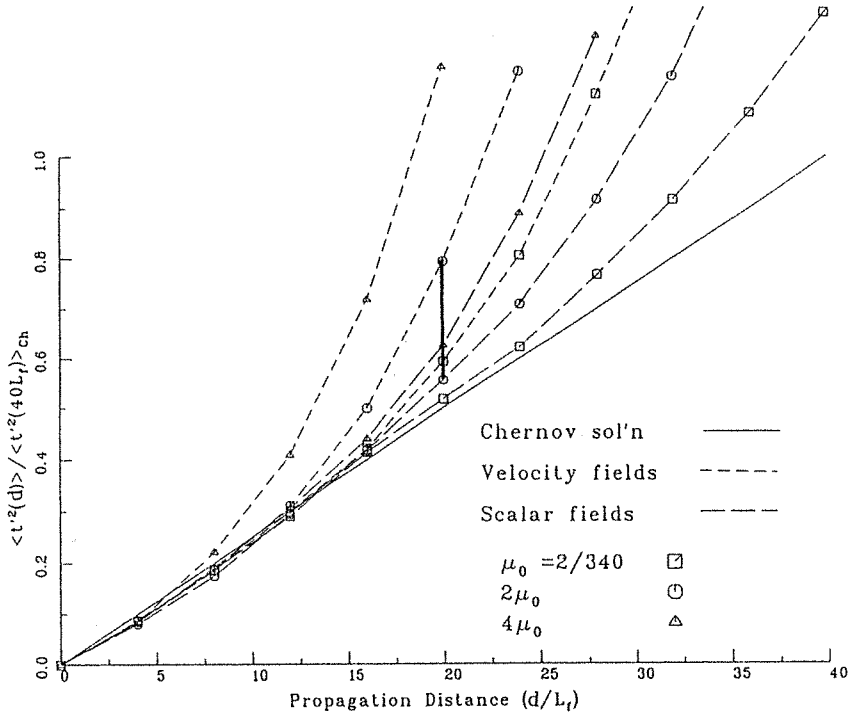

Fig. 1. — Travel-time variance $\langle t'^2(d) \rangle$ for rays propagating through isotropic temperature (scalar) and velocity fields having different perturbation indices $\mu=\mu_0$, $2\mu_0$, $4\mu_0$, but identical integral length scales $L_f=0.1\sqrt{\pi}/2$. Results are normalized with respect to the Chernov solution at a distance $d=40\ L_f$. The difference between the $\langle t'^2 \rangle s$ for temperature and velocity fields at $d=20\ L_f$ for $2\mu_0$ is accented by a heavy vertical line.

Fig. 1. — Evolution de la variance $\langle t'^2(d) \rangle$ avec la distance pour une onde acoustique se propageant dans des champs turbulents isotropes scalaire ou vectoriel ($\mu=\mu_0$, $2\mu_0$, $4\mu_0$ et $L_f=0{,}1\sqrt{\pi}/2$). Pour $d=20\ L_f$ et $2\mu_0$, la différence entre les cas thermique et cinématique est indiquée par une ligne verticale.

Figure 1 shows travel-time variance as a function of propagation distance for the three scalar and three vector cases. Results are normalized by the Chernov prediction at a distance of $d=40\ L_f$. Since the Chernov formula takes into consideration the perturbation index, and all the fields have the same longitudinal integral length scale, we might have expected similar time-variation behaviour. But the results are clearly quantitatively different. For example, for a perturbation index of $2\mu_0$ at $d/L_f=20$, the scalar-field time variation exceeds the Chernov result by only 10%; whereas the velocity-field time variation exceeds it by 60%. (This difference is indicated by a heavy vertical line on the figure.) The departures from the Chernov prediction increase with perturbation index and travel distance. The effect of travel distance has previously been observed by Karweit (1991) for velocity fields.

Karweit (1991) also observed that when the phase point in a velocity field was constrained to follow an axial trajectory, its time variation matched the Chernov result. Since it is the lateral gradients of the velocity (temperature) that bend trajectories from their original directions, our second set of experiments focused on the lateral characteristics of the perturbation fields. In what follows, we assume that the axial direction is x_1

and axial distances are expressed as r_1. Lateral or transverse distances are referenced as r_T; or as r_2 or r_3 in cartesian directions. And, $r=\|\mathbf{r}\|$.

It is the smaller scales of inhomogeneities which contribute most to gradients. A simple measure of these scales in the Taylor microscale λ_i where

$$\frac{1}{\lambda_i^2}=-\frac{1}{2}\frac{\partial^2\rho(\mathbf{r})}{\partial r_i^2}, \quad \text{at } \mathbf{r}=0. \tag{7}$$

What may be the significant difference between ray propagation in isotropic velocity fields and ray propagation in isotropic temperature fields with the same longitudinal integral length scale L_f and correlation function of inhomogeneities $\rho(r)$ is that their resulting perturbation fields will have the same longitudinal Taylor microscale λ_1, but will have different lateral Taylor microscales λ_2.

An isotropic temperature field is itself a scalar perturbation field whose correlation of spatial inhomogeneities can be expressed as $\rho(r)$, so that $\lambda_1=\lambda_2=\lambda_3$. But when an isotropic velocity field is evaluated as a scalar perturbation field for acoustic propagation in, say, the x_1 direction where only the u_1 velocity component plays a role, the correlation of spatial perturbations becomes axisymmetric about x_1 and must be expressed as $\rho(r_1, r_T)$. This is an artefact of a continuity constraint between components of velocity, which of course does not exist for a temperature field. For isotropic fields, this constraint defines a relationship between lateral and axial correlations as:

$$f(r)+\frac{r}{2}\frac{\partial f}{\partial r}=g(r). \tag{8}$$

where $f(r)$ and $g(r)$ are the Karman-Howarth longitudinal (axial) and lateral correlation functions. With x_1 the direction of acoustic propagation, the relationship between the Taylor microscales is $\lambda_2=\lambda_3=\lambda_1/\sqrt{2}$. [*See* Hinze (1975).] The net result is that λ_2 for our velocity fields is $\sqrt{2}$ times smaller than λ_2 for our temperature fields.

To assess the importance of lateral scales, we created axisymmetric scalar fields about x_1 whose longitudinal integral length scale and lateral microscales matched those of the isotropic velocity fields. Here the spatial correlation of the fluctuations is expressed as $\rho(r_1, r_T)$, a function of both lateral and longitudinal separations. Following the rapid distortion theory of Batchelor (1953) for velocity fields, we assumed our initially-isotropic scalar fields were suddenly forced through a contraction with contraction parameter C. This results in the following relationships between the original field scale l and the contracted field scales L_1, L_2, L_3:

$$L_1^2=C^2 l^2, \qquad L_2^2=L_3^2=l^2/C \tag{9}$$

$$\frac{\partial^2\rho}{\partial r_1^2}\Big/\frac{\partial^2\rho}{\partial r_2^2}=\frac{1}{\lambda_1^2}\Big/\frac{1}{\lambda_2^2}=L_2^2/L_1^2=1/C^3 \tag{10}$$

Choosing $C=2^{1/3}$ gives a $\sqrt{2}$ ratio of longitudinal to lateral scales—the same as for a velocity field. To provide an integral scale of $L_f=0.1\sqrt{\pi}/2$ for the now axisymmetric temperature field, the length parameter is prescribed as $l=0.1/C$.

Once more, following the trajectories of rays through ensembles of these axisymmetric scalar fields, we accumulated time-variance statistics for direct comparison with the analogous velocity fields. Figure 2 shows the results along with the velocity curves of figure 1. Here, the axisymmetric scalar results now lie much closer to those of the comparable velocity experiments. Using the same example as before (*i.e.* $2\mu_0$ at $d/L_f=20$), we observe (heavy vertical line) that the excess of time variance over the

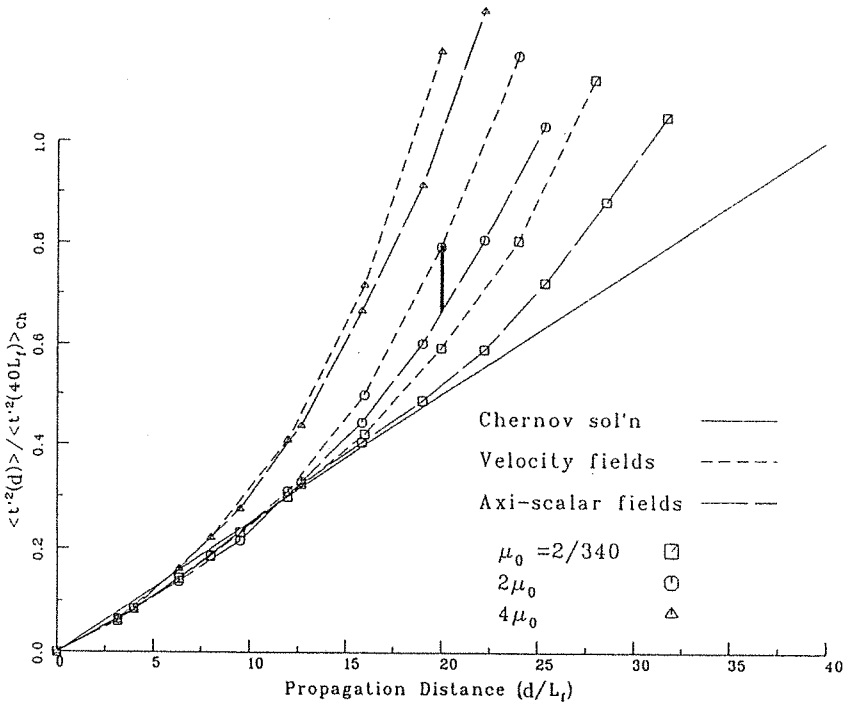

Fig. 2. – Travel-time variance $\langle t'^2(d) \rangle$ for rays propagating through isotropic velocity fields and axisymmetric temperature (scalar) field where both the integral length scales L_f and the lateral Taylor length scales associated with the perturbation field λ_2 are matched. Plots are presented for three values of the perturbation index $\mu = \mu_0, 2\mu_0, 4\mu_0$. Results are normalized as in figure 1. The difference between the $\langle t'^2 \rangle s$ for isotropic velocity and axisymmetric temperature fields at $d = 20\,L_f$ for $2\mu_0$ is accented by a heavy vertical line.

Fig. 2. – Evolution de la variance $\langle t'^2(d) \rangle$ avec la distance pour une onde acoustique se propageant dans un champ vectoriel isotrope et dans un champ scalaire axisymétrique ayant les mêmes échelles L_f et λ_2 pour trois valeurs des fluctuations d'indice $\mu = \mu_0, 2\mu_0, 4\mu_0$. Pour $d = 20\,L_f$ et $2\mu_0$, la différence entre les deux simulations est mise en évidence par une ligne verticale.

Chernov result is now 35% in comparison with the velocity field's 60%. Recall that the excess for scalar fields with non-comparable λ_2 was only 10%. Thus, we must conclude that lateral scales cannot be neglected when one estimates travel time-variance or phase variance in high-frequency acoustic propagation. From figure 2, we also remark that the comparability between similar velocity and axisymmetric scalar fields appears to improve with increasing perturbation index.

In this paper we have clearly demonstrated a significant difference between isotropic scalar and vector fields with respect to their effect on acoustic propagation. Also, this difference was found to relate to their respective lateral scales. A consequence of this finding is that the classical result of Chernov, which ignores the effect of lateral scales, should not be relied upon to yield an accurate prediction of phase variance in inhomogeneous media.

It remains to deduce a better influence of these lateral scales than simply λ_2. At present we are examining the 2-D numerical experiments of Blanc-Benon (1991) to see if the lateral scales associated with caustics can be applied to the current problem of phase dispersion.

Note remise le 21 avril 1993, acceptée le 4 mai 1993.

References

G. K. BATCHELOR, *The Theory of Homogeneous Turbulence*, Cambridge, Cambridge, 1953.

Ph. BLANC-BENON, D. JUVÉ, M. KARWEIT and G. COMTE-BELLOT, Simulation numérique de la propagation des ondes acoustiques à travers une turbulence cinématique, *J. Acoust.*, 3, 1, 1990, pp. 1-8.

Ph. BLANC-BENON, D. JUVÉ and G. COMTE-BELLOT, Occurrence of caustics for high frequency acoustic waves propagating through turbulent fields, *Th. and Comp. Fluid Dyn.*, 2, 1991, pp. 271-278.

S. CANDEL, Numerical solution of conservation equations arising in linear wave theory: application to aeroacoustics, *J. Fluid. Mech.*, 83, 1977, pp. 465-493.

S. CANDEL, Numerical solution of wave scattering problems in the parabolic approximation, *J. Fluid. Mech.*, 90, 1979, pp. 465-507.

L. CHERNOV, *Wave Propagation in a Random Medium*, McGraw-Hill, New York, 1960.

M. KARWEIT, Ph. BLANC-BENON, D. JUVÉ and G. COMTE-BELLOT, Simulation of the propagation of an acoustic wave through a turbulent velocity field: A study of phase variance, *J. Acoust. Soc. Am.*, 89, (1), 1991, pp. 52-62.

J. O. HINZE, *Turbulence*, McGraw-Hill, New York, 1975.

A. D. PIERCE, *Acoustics: An Introduction to Its Physical Principles and Applications*, McGraw-Hill, New York, 1981.

M. K. : *Dept. Chemical Engineering, Johns Hopkins University, Baltimore, MD.* 21218, *USA;*

Ph B.-B. : *Laboratoire de Mécanique des Fluides et d'Acoustique, URA-CNRS No.* 263, *École Centrale de Lyon*, BP No. 163, 69131 *Ecully Cedex, France.*